



## Soil Science and Agricultural Engineering

Available online at <http://zjar.journals.ekb.eg>  
<http://www.journals.zu.edu.eg/journalDisplay.aspx?JournalId=1&queryType=Master>



## COPPER REMOVAL FROM AQUEOUS SOLUTION OF CONTAMINATED SOIL USING NATURAL ZEOLITE

Ahmed S. Abd-Elaziz<sup>1\*</sup>, M.S. Atress<sup>1</sup>, E.A. Haggag<sup>1</sup> and K.G. Soliman<sup>2</sup>

1. Nuclear Materials Authority, P.O. Box 530 Maadi, Egypt

2. Soil Sci. Dept., Fac. Agric., Zagazig Univ., Egypt

Received: 28/11/2022 ; Accepted: 30/08/2023

**ABSTRACT:** Natural zeolite is used as an inexpensive sorbent to remove copper from water. The factors that affect adsorption include contact time, temperature during adsorption, starting copper concentration, and S/L ratio. Zeolite from an acidic media has been studied to identify its equilibrium and kinetic properties. This investigation's goal was to assess the removal of copper using various solutions and the adsorption of copper from pre-contaminated soil. Metals were removed from the soil by washing with organic weak acids such as citric, maleic, succinic, tartaric, lactic, and oxalic. The surface layer (0–30 cm) of the soil was sampled in the field of Inchass, Sharkia Governorate, Egypt. 100 ppm copper citrate was present in the soils as a pre-contaminant. To test the copper's ability to leach effectively, mild organic acids were applied in concentrations ranging from 0.5% to 3.0%. Under ideal circumstances, it has been discovered that the realistic capacity of copper to adsorb onto zeolite can reach 32 mg/g, which corresponds to the 32 mg/g Langmuir isotherm. The nature of the copper adsorption by the natural zeolite has also been determined using physical characteristics, such as adsorption kinetics, isotherm models, and thermodynamic data. The Langmuir isotherm and the pseudo-second-order reaction were both found to be in agreement with the functional natural zeolite.

**Key words:** Copper removal, leaching agent, natural zeolite, adsorption isotherms.

### INTRODUCTION

According to Liu *et al.* (2013), Copper is one of the most pervasive pollutants in the water environment around industrial facilities like metal finishing, electroplating, fertilizer, mining operations and paint. According to several studies (Chauhan *et al.*, 2000; Zhao *et al.*, 2010; Zhu *et al.*, 2011; Wu *et al.*, 2011), Through the water cycle, an excessive amount of copper would accumulate in the organism and cause nausea, vomiting, and perhaps movement and neurological abnormalities. To lessen the threat that copper poses to the environment, it is crucial to properly remove Cu(II) from contaminated aqueous solutions. Due to its high effectiveness, ease of use, and low cost, the sorption method is one of many purifying technologies that has attracted interest. several adsorbents, including oxides (Kim *et al.*, 2003),

There have been numerous methods proposed for the purification and remediation of contaminated water bodies, including porous material (Ren *et al.*, 2012), chelating resin (Zhu *et al.*, 2015), and chelating reagent (Kryvoruchko *et al.*, 2004; Mellah *et al.*, 2006; Gupta and Rastogi, 2008; Kadous *et al.*, 2009; Zou *et al.*, 2011). However, restrictions including high cost and environmental toxicity limited further industrial uses. difficult synthesis procedure, and subpar removal performance. As a result, a sorbent that is extremely efficient, economical, and eco-friendly was developed to remove copper contaminants from aqueous solutions. (Kocaoba *et al.*, 2007; Perić *et al.*, 2004; Babel and Kurniawan, 2003; Sprynskyy *et al.*, 2006; Loizidou and Townsend, 1987; Shadbad *et al.*, 2011). Recently, emphasis has been placed on the use of alternative, inexpensive materials as potential sorbents to remove heavy metals.

\* Corresponding author: Tel. :+201096593691

E-mail address: Ahmedsf@gmail.com

Natural zeolite is an aluminosilicate mineral that has a wide surface area, significant ion exchange and adsorption capabilities due to its unique tetrahedral pore structure. Additionally, they are inexpensive and accessible materials that have been employed for heavy metal adsorption. (Kilincarslan and Akyil, 2005; Sharma and Tomar, 2008; Krestou et al., 2003; Akyil et al., 1998; Ames et al., 1983). High stability constants and resistance to radiation damage make framework-structured zeolite an ideal inorganic ion exchanger. The goal of the current study was to evaluate zeolite's abilities to adsorb copper ions from synthetic solutions. On the adsorption of copper ions, the impacts of several factors, including the starting pH, the initial concentration of copper ions, and the presence of salt, were examined. The goal of the current work is to assess how well various organic acids may leach copper from pre-contaminated soils as well as how well some weak organic acids can leach copper from pre-contaminated soils.

## MATERIALS AND METHODS

### Soils

Soil used in the experiment was collected from the surface layers (0 – 30 cm) of a field in Inchass Area, Sharkia Governorate, Egypt. The soil was a sandy loam that was taken from field under arable cultivated, and irrigated by sewage water for about 80 years. Some physical and chemical characteristics of soil from Inchass area are shown in Table 1.

### Leaching of Contaminated Soil

Water was acidified with phosphoric acid until pH 2 or water was used for the soil leaching test. Also, six organic acids namely; lactic, tartaric, succinic, maleic, oxalic, and citric acids, were used for soil washing test.

### Chemicals and Reagents

All chemicals used for analysis were analytical-grade reagents. Copper sulfate pentahydrate  $\text{CuSO}_4 \cdot 5\text{H}_2\text{O}$  from IBI labs, Florida, USA and HCl 37%,  $\text{HNO}_3$ , NaCl.

### Preparation of the Pregnant Solutions

- The samples used in this experiment were typically weighed using a Shimadzu (AY 220) analytical balance.

- Hot plate magnetic stirrer model Fisher Scientific.
- The pH-meter model (HAANA pH-mV-temp) was used to precisely measure the hydrogen ion concentration in the various solutions.
- Cuprizone reagent (Sigma-Aldrich) was used to do the quantitative examination of copper using a UV-spectrophotometer, the "single beam multi-cells-positions model SP-8001" from Metretech Inc. (Marczenko and Balcerzak, 2000; Haggag et al., 2021a; Khawassek et al., 2016; Moussa et al., 2014).

## Experimental Procedure

The basic equilibrium conditions for copper adsorption, including pH, contact time, temperature, and the ratio of natural zeolite to liquid, were optimized using the batch technique. In these tests, a 100 ml conical flask containing 10 ml of a 100 mg/L Cu solution was swirled at 250 rpm with 0.05 g of dry natural zeolite. The zeolite and liquor were combined, the two phases were decanted, and the clear raffinate's copper content was assessed. Equation (1) was used to compute the quantity of copper adsorption  $q_e$  (mg/g) from the difference in copper concentration in the aqueous solution before and after adsorption at the equilibrium period t:

$$q_e = (C_o - C_e) \frac{V}{m} \quad (1)$$

Where  $C_o$  and  $C_e$  are the initial and equilibrium concentrations of copper in the solution ( $\text{mol. L}^{-1}$ ),  $V$  is the volume of solution ( $\text{mol. L}^{-1}$ ), ( $L$ ) and  $m$  is the weight of the zeolite (g).  $V$  is the volume of solution.

$$\text{Cu \%} = \frac{(C_o - C_e)}{C_e} \times 100 \quad (2)$$

Equation (3) was used to compute the distribution coefficient ( $K_d$ ) of copper between the solid phase zeolite and the aqueous bulk phase:

$$K_d = \frac{C_o - C_e}{C_e} \times \frac{V}{m} \quad (3)$$

## Optimization of the Leaching Process

It was concluded that the leaching potentialities of these crucial metal values needed to be explored because of the numerous mineral elements in the research ore sample.

**Table 1. Some physical and chemical characteristics of soil from Inchass area**

Characteristic	Value
<b>Particle size distribution, %</b>	
Sand	73.4
Silt	12.5
Clay	14.1
<b>Texture class</b>	Sandy loam
OM, %	1.61
CaCO <sub>3</sub> , %	2.55
pH	8.20
EC, dS/m	0.62
<b>Soluble ions, mmole/l</b>	
Ca <sup>++</sup>	0.06
Mg <sup>++</sup>	0.16
Na <sup>+</sup>	0.04
K <sup>+</sup>	0.12
CO <sub>3</sub> <sup>--</sup>	--
HCO <sub>3</sub> <sup>-</sup>	0.01
Cl <sup>-</sup>	0.03
SO <sub>4</sub> <sup>--</sup>	0.22
<b>Total content, µg/g</b>	
Cu	13
Ni	11

## RESULTS AND DISCUSSION

### Effect of Parameters

In the section that follows, the outcomes of dissolving polluted soil using citric acid solution are discussed. This study examined the impact of reaction duration, citric acid concentration, solid to liquid ratio, and temperature on the dissolution process.

### Effect of Organic Acids Types

Investigated was how various organic acid types affected the amount of copper leaching from polluted soil. 1.0 M organic acid type concentration, 63 µm particle size, room temperature, 600 rpm stirring speed, 120 min stirring time, and 1:10 g/ml S/L mass ratio were used as fixed parameters, it was determined how different types of organic acids affected copper leaching from contaminated soil. According to the experimental findings between copper leaching efficiency and organic acid type shown in Fig. 1, the following organic acids have an impact on the amount of copper that is

leached: citric acid (81.3% Cu), tartaric acid (46.8% Cu), succinic acid (20.3% Cu), maleic acid (28.8% Cu), and oxalic acid (40.4% Cu). Citric acid is therefore the preferred acid for the studies that follow to dissolve polluted soil (**Khawassek et al., 2015**).

### Effect of Citric Acid Concentration

Cu from contaminated soil was examined using a solid/liquid ratio of 1:10 g/ml at room temperature with a stirring speed of 600 rpm and 63 µm particle size. Citric acid concentration ranged from 0.2 to 1.4 M. According to the findings in Fig. 2, which depict a relationship between copper leaching efficiency and citric acid concentration, copper leaching efficiency increased from 24.0 to 80.3% when citric acid concentration increased from 0.2 to 1.0 M. The increase in H<sup>+</sup> ions in the solution may be the cause of this. A further increase in citric acid has a small impact on the proportion of copper leaching. As a result, the preferred acid concentration for the remaining tests involving the dissolving of the working material is 1.0 M citric acid (**Zafar and Ashraf, 2007**).

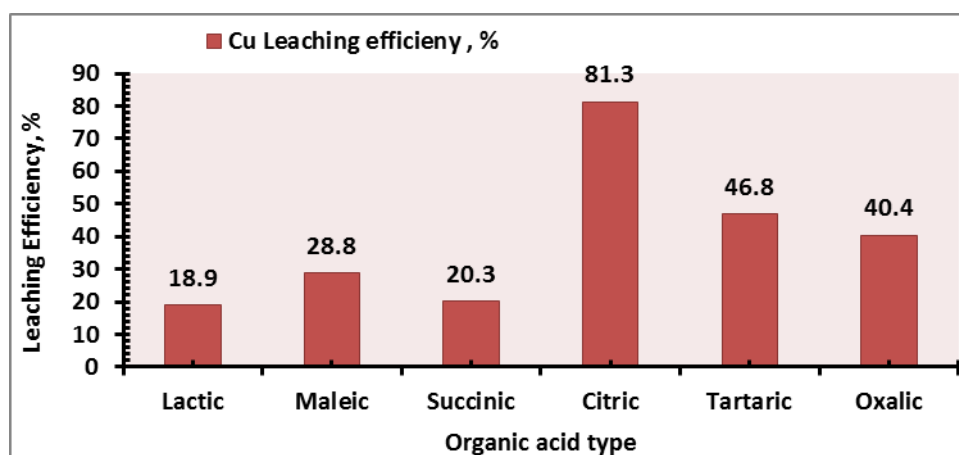


Fig. 1. Effect of organic acid types on the effectiveness of dissolving copper, % (S/L mass ratio: 1:10 g/ml; temperature: 25°C; particle size: 63 m; [Organic acid]:1.0 M; stirring time: 120 min;)

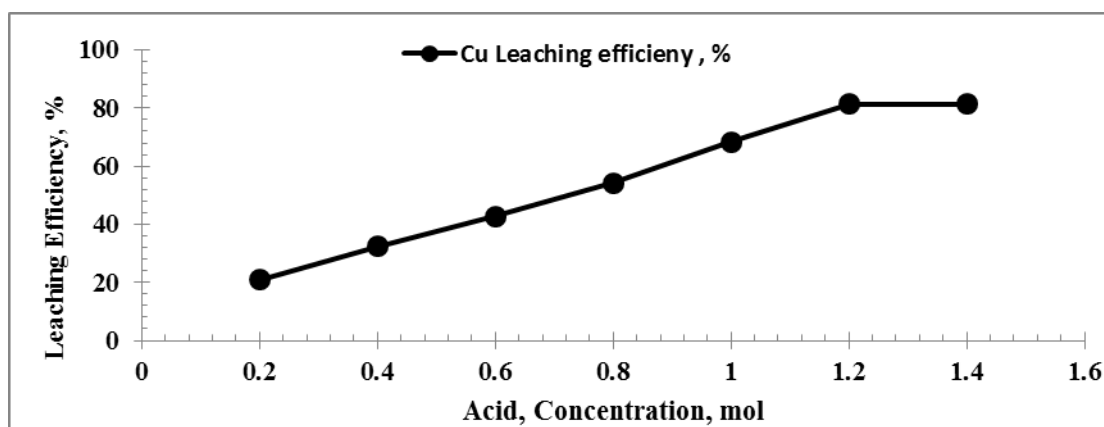


Fig. 2. Effect of citric acid concentration on copper dissolving efficiency, percent (temperature: 25°C; particle size: 63 m; stirring time: 120 min; S/L mass ratio: 1:10 g/ml; stirring speed: 600 rpm)

### Effect of Reaction Time

A time range of 15 to 240 minutes, 600 rpm stirring, 1M citric acid concentration, room temperature, 63 m particle size, and a solid/liquid ratio of 1:10g/ml were used to study this factor. The experimental results, which are represented in Fig. 3 as a function of reaction time, demonstrate that as the reaction duration rose from 15 to 180 min, the copper leaching percentage increased by roughly 8.0 to 78.0%. The effectiveness of copper leaching is only slightly affected by increased stirring time of more than 180 minutes. The reaction dissolution time was set at 180 minutes in all following experiments based on the findings (Gharabaghi *et al.*, 2009).

### Effect of Particle Size

Six distinct particle sizes-400 m, 300 m, 149 m, 100 m, 63 m, and 32 m-were used to test the impact of particle size on copper leaching. According to Fig. 4, the copper leaching efficiency rose from 14.0 to 86.0% when the working ore's particle size fell from 400 to 63 m. Conversion rates are inversely correlated with average initial particle diameter because the lowest particle size fraction has the most surface area. The effectiveness of copper leaching is very slightly impacted by increased particle size of more than 63 m. Consequently, 63 m was the recommended particle size (Puigdomenech, 2006).

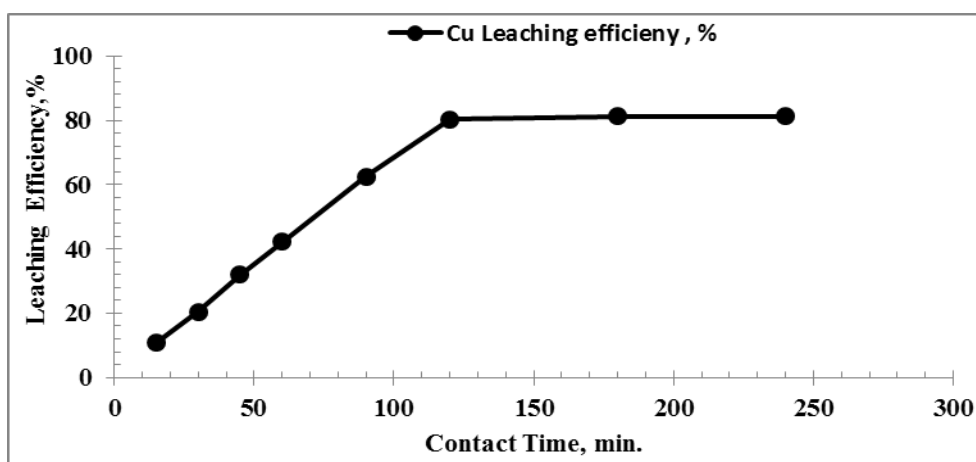


Fig. 3. Effect of Effect of reaction time on copper dissolution efficiency, % (temperature:  $25 \pm 1^\circ\text{C}$ ; particle size:  $63 \mu\text{m}$ ; [Citric acid]: 1.0 M; S/L mass ratio: 1:10 g/ml; stirring speed: 600 rpm)

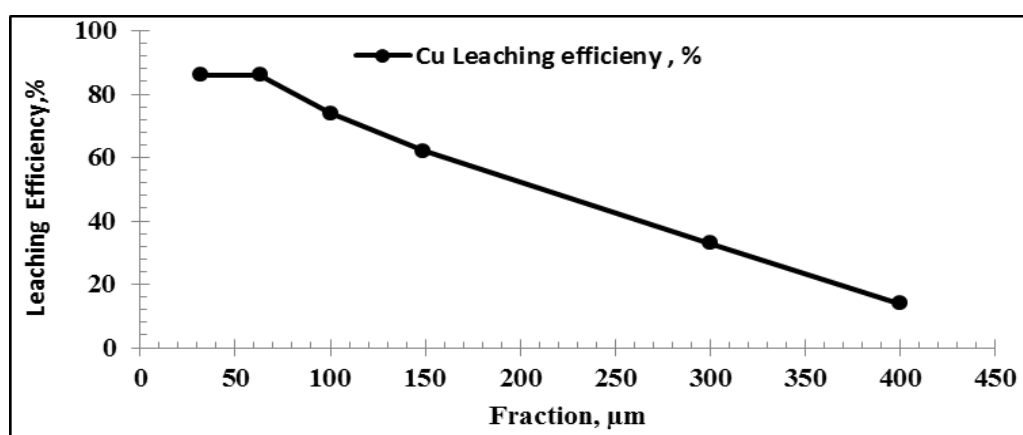


Fig. 4. Efficiency of copper dissolving as a function of particle size,% (room temperature; 1 M citric acid; 120 min of stirring; 1:10 g/mL S/L mass ratio; 600 rpm)

### Effect of Solid/Liquid Ratio

Fig. 5 illustrates the effect of the solid/liquid ratio on copper dissolving under the following conditions: reaction time of 120 min; stirring rate of 600 rpm; acid concentration of 1.0 M at room temperature; and particle size of 63 m. When the solid/liquid ratio was raised from 1 to 20 g/ml, the experimental findings consistently demonstrated an increase in copper from 20.0 to 86.00%. This could be explained by the fact that when the solution's bulk density increases, the migration of copper ions into the liquid medium decreases. More than 1:10 g/ml increases in the material to liquid ratio rarely have an impact on leaching efficiency. Therefore, the ideal setting

for the other dissolving investigations is 1:10 g/ml ore/citric acid (Haggag *et al.*, 2021b).

### Effect of Temperature

The effect of reaction temperature on the dissolving process was examined using a reaction time of 120 minutes, a stirring speed of 600 rpm, a citric acid concentration of 1.0 M, a particle size of 63 m, and a solid/liquid ratio of 1:10 g/ml. According to Fig. 6, , the copper leaching efficiency increased from 82.0 to 90.0% as the working ore's temperature rose from 25 to  $50^\circ\text{C}$ . Cu was more effectively dissolved by raising the reaction temperature from 25 to  $50^\circ\text{C}$ . Therefore,  $50^\circ\text{C}$  is the ideal temperature for the studies involving the other components (El-Sheikh *et al.*, 2020).

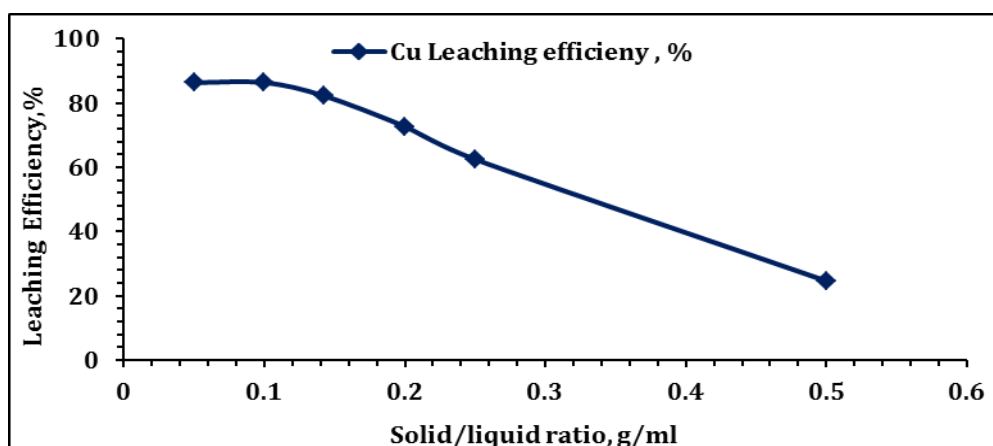


Fig. 5. Effect of solid/liquid ratio on copper dissolution efficiency, % (stirring speed: 600 rpm; temperature: 60°C, particle size: 63  $\mu\text{m}$ ; [Citric acid]: 1.0 M; stirring time: 120 min)

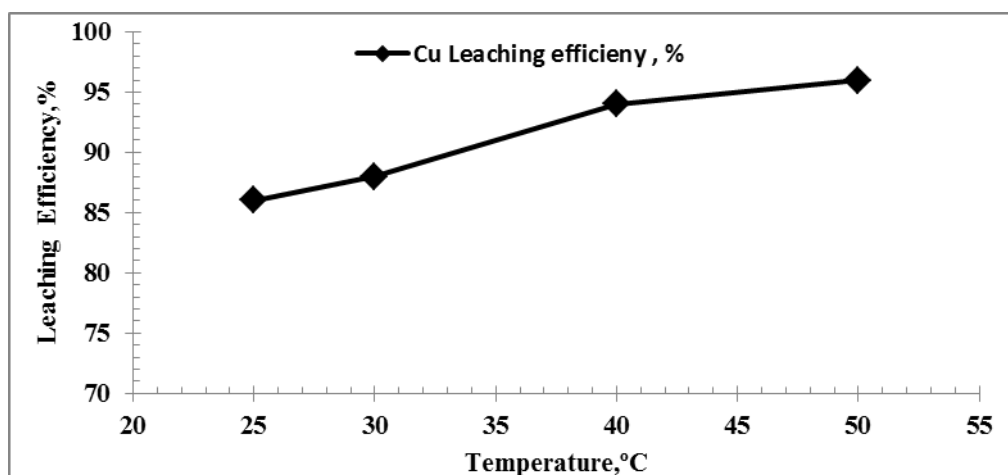


Fig. 6. Effect of reaction temperature on copper dissolution efficiency, % (stirring speed: 600 rpm; particle size: 63  $\mu\text{m}$ ; S/L mass ratio: 1:10 g/ml; stirring time: 120 min; [Citric acid]: 1.0 M)

### Preparation of Pregnant Leach Liquor from Contaminated Soils

The recommended leaching conditions (1.0 M citric acid, 180 min of agitation, S/L of 1/10, grain size 63  $\mu\text{m}$ , stirring speed 600 rpm at ambient temperature) were used in a thorough study on 5.0 kg of contaminated soils, and copper concentrations of 100 mg/L were measured. The pH was found to be 1.0, and it was then corrected by adding 10% NaOH solution to the adsorption system. In this investigation, the batch stirring adsorption method was used. Copper was removed from leach liquor using natural zeolite (NZ). Using natural zeolite, copper adsorption from the pregnant citrate leach fluid was thoroughly investigated (Dacrory *et al.*, 2020).

### Conditions for Copper Adsorption optimized.

#### Effect of pH

The pH of a solution has a significant impact on copper adsorption because it affects both the degree of ionization (speciation) and the surface charge of NZ (Mahmoud *et al.*, 2015). In Fig. 7, it was examined how pH affected the effectiveness of copper being adsorbed from citrate solutions with various pH values (ranging from 0.4 to 4.5). The obtained data demonstrate that the adsorption effectiveness rose as the pH value climbed, reaching 70.0% when the solution's pH was raised to 2.5, which is considered to be the ideal pH. In Fig. 8, copper's speciation distribution (degree of ionization) in citrate media was taken into consideration and described.

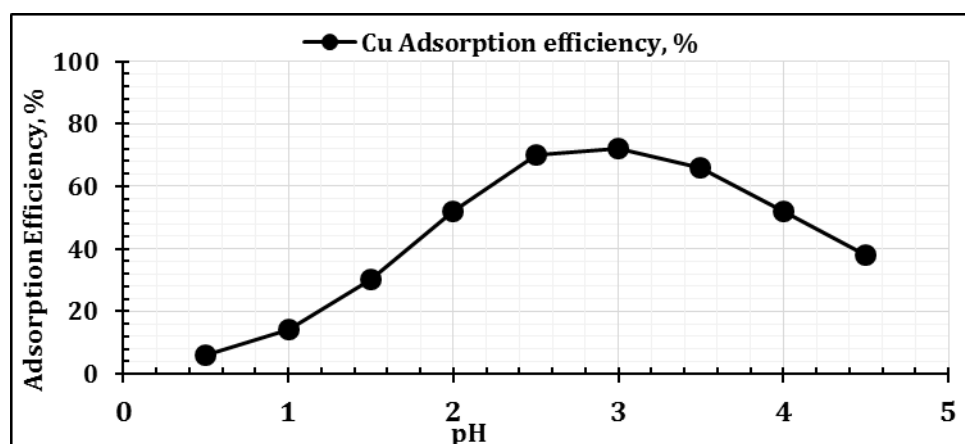


Fig. 7. Effect of pH on the adsorption of copper ( $C_0$ :  $100 \pm 5$  mg L<sup>-1</sup>; contact time: 60 min; T:  $25 \pm 1^\circ\text{C}$ , rpm: 250, NZ weight: 0.05 g)

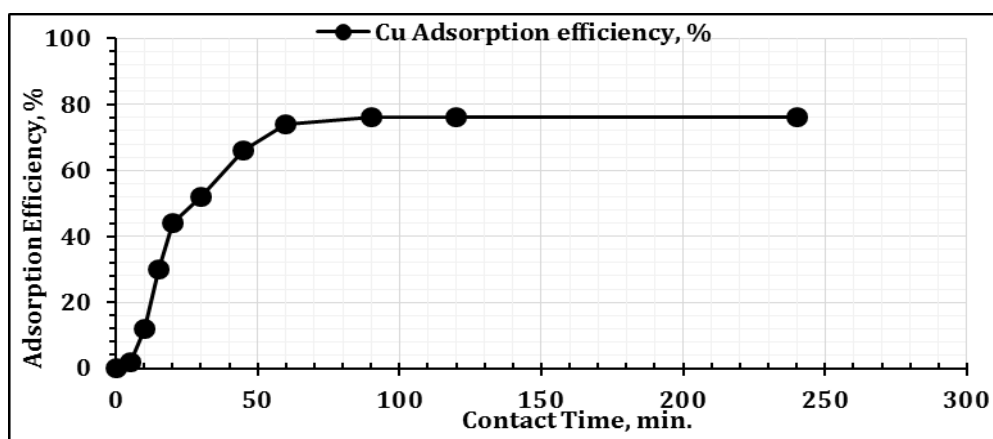


Fig. 8. Effect of contact time on the effectiveness of copper adsorption onto NZ (T:  $25 \pm 1^\circ\text{C}$ ; NZ weight: 0.05 g, Cu conc.: 100 mg/L, volume: 10 ml, rpm: 250, pH: 3.0)

#### Effect of contact time

The test ranged from 5 to 240 minutes using 10 ml of nitrate solution evaluating 100 mg Cu/L, while the other conditions were kept at pH 2.5 and 0.05 g NZ at room temperature. The effect of contact duration on the effectiveness of copper adsorption was evaluated. As shown in Fig. 9, which compiles the outcomes, From 5 to 240 minutes of contact time, copper's adsorption effectiveness increased visibly; the maximum adsorption efficiency (76.0%) was obtained after 90 minutes. It was decided that the equilibrium adsorption time would be 90 minutes. The interval adsorption method did not alter as reaction contact time increased. This can indicate a downturn. The interval adsorption method has not changed despite an increase in reaction contact time. This might be related to a drop in the number of NZ

active sites and a drop in the amount of copper in the solution. (Abdel-Samad *et al.*, 2020).

#### Effect of temperature

With a reaction time of 90 minutes, 10 mL of copper with a concentration of 100 mg/L at a solution pH of 2.5, and 0.05g NZ, the influence of temperature on copper adsorption from synthetic citrate solution was investigated. According to the findings in Fig. 10, the copper adsorption reduced as the temperature rose from 25 to 50°C, going from roughly 61.6 to 50%. 25°C was shown to be the ideal adsorption temperature for extracting copper from citrate solution using NZ. The chosen reaction temperature is represented by the room temperature according to the results (Haggag *et al.*, 2019).

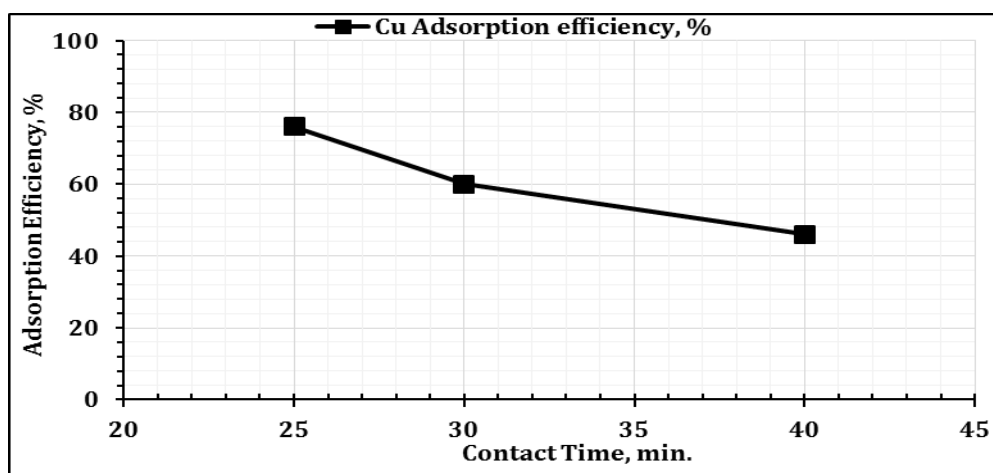


Fig. 9. Effect of temperature on the effectiveness of copper adsorption (contact time: 90 min; NZ weight: 0.05 g, Cu conc.: 100 mg/L, volume:10 ml; pH:3.0, rpm: 250)

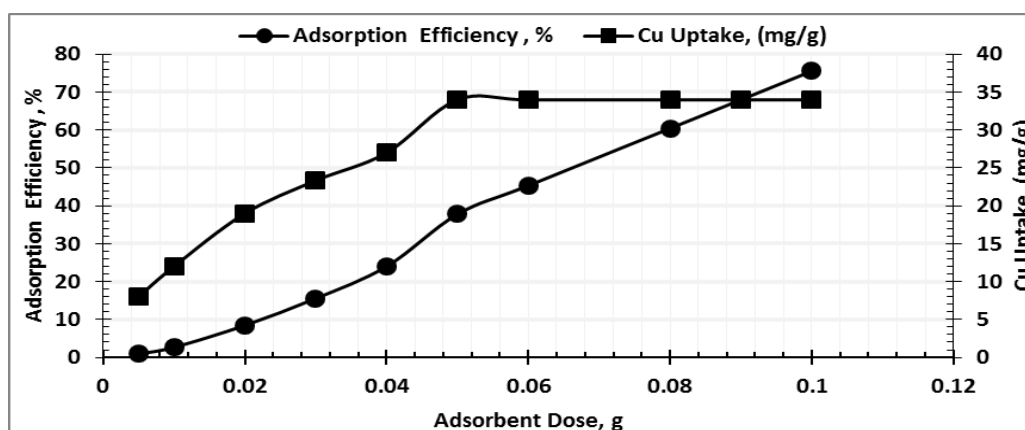


Fig. 10. Effect of NZ dose on adsorption of copper (T:25 ± 1°C; contact time: 90 min; volume:10 ml; pH:3.0, Cu conc.: 100 mg/L; rpm: 250)

#### Effect of NZ dosage

The impact of adsorbent dose on copper adsorption efficiency and copper absorption rate was examined for 120 minutes under the following conditions: the NZ weight was between 0.005 and 0.1 g, the copper concentration was 100 mg/l, and the pH value was 2.5.

The experimental results, as shown in Fig. 10, demonstrated that increasing the adsorbent dose from 0.005 to 0.1 g significantly increased the efficacy of copper adsorption. Due to the solution's low copper concentration, an additional increase in NZ dosage of 0.08 to 0.1 g was unable to result in significant elimination. The increase in adsorption active sites and NZ surface area can be used to identify this phenomenon. At

an adsorbent dosage, the highest copper removal effectiveness of 32.0% was achieved (Thanavel et al., 2019).

#### Effect of initial copper concentration

As a function of the starting copper concentration from 50 to 500 mg/L at a pH value of 2.5 for 90 min and using 0.05 g NZ at room temperature, the copper adsorption effectiveness of NZ was investigated. According to Fig. 11. it was discovered that when copper concentration grew from 50 to 500 mg/l, the effectiveness of copper adsorption fell from 95.0 to 52.8% while copper uptake increased from 7.6 to 34.0 mg Cu/g. Due to the copper ions' affinity to connect with the active sites after the first increase in copper concentration, this drop



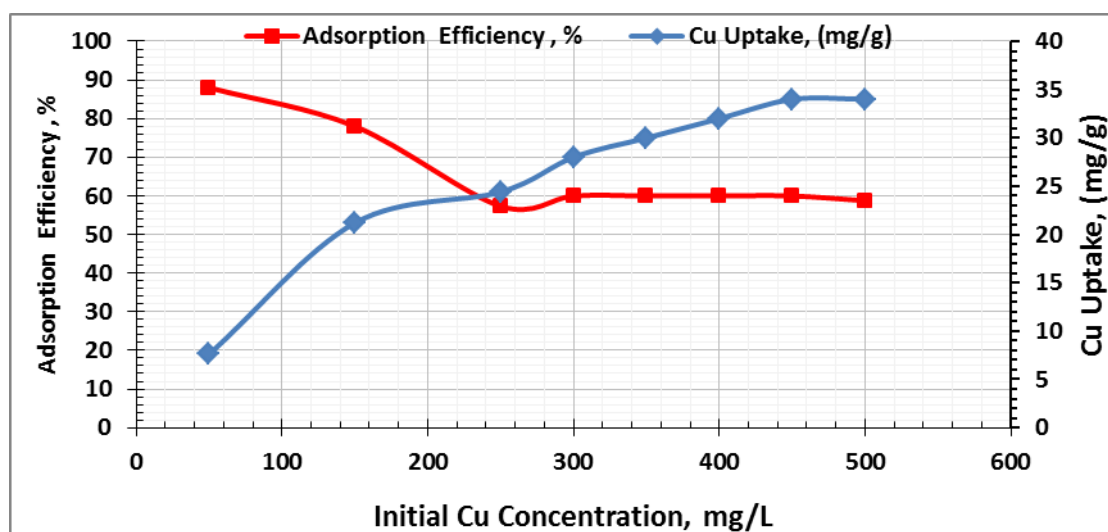


Fig. 11. Effect of initial copper concentration on copper adsorption efficiency onto NZ (T:25 ± 1°C; contact time: 90 min; NZ weight: 0.05 g, volume:10 ml; pH:3.0, rpm:250)

in adsorption efficiency can be explained by the decrease in the number of active sites on NZ (Khawassek *et al.*, 2017). Thus, the maximum saturation capacity of NZ was maintained at 34.0 mg Cu/g NZ.

### Adsorption Kinetics and Mechanism

The adsorption mechanism was examined using the kinetic models. The rate-controlling phase of the adsorption interactions was described using the adsorption kinetics studies and mechanisms as a function of temperatures (25 - 40°C) and estimated by pseudo-first-order (Lagergren equation) and pseudo-second-order models. Two or more equation models were used to evaluate the results of batch tests in order to determine the rate of the adsorption interactions (Lagergren, 1898; Espinoza-Sanchez *et al.*, 2019).

$$\text{Log}(q_e - q_t) = \text{Log}q_e - \left(\frac{K_1}{2.303}\right)t \quad \text{Pseudo-first-order}$$

Where  $q_t$  and  $q_e$  are, respectively, the amounts of copper adsorbed at equilibrium time (240 min.) and at a specific time  $t$  (mg/g). As shown in Fig. 12A, equilibrium adsorption capacity  $q_e$  (mg/g) and pseudo-first-order rate constant  $K_1$  (min<sup>-1</sup>) were determined from the intercept and slope of the plot  $\text{log}(q_e - q_t)$  against  $t$  for copper adsorption at various temperatures. The correlation

coefficient ( $R^2$ ) values for the pseudo-first-order kinetic are given in Table 2 and vary from 0.962 to 0.588. The calculated maximal adsorption capacity ( $q_{\text{ecal}}$ ) also differs greatly from the actually achieved capacity ( $q_{\text{exp}}$ ). Application of pseudofirst order mechanism data to NZ's adsorption of copper revealed that it did not fit.

$$\frac{t}{q_t} = \frac{1}{K_2 q_e^2} + \left(\frac{1}{q_e}\right)t \quad \text{Pseudo-second-order}$$

The pseudo-second-order rate constant  $K_2$  (min<sup>-1</sup>) and the equilibrium adsorption capacity  $q_e$  (mg/g) were calculated experimentally using the slope and intercept of the plot of  $t/q_t$  versus  $t$  shown in Fig. 12 B. At various temperatures, the pseudo-second-order plot shows good linearity and straight lines. The experimental equilibrium adsorption capacity ( $q_{\text{exp}}$ ) of copper over NZ at 25, 30, and 40°C was 15.52, 12.0, and 8.31 mg/g, respectively, as indicated in Table 2. Additionally, for all concentrations at the four distinct temperatures, an extraordinarily high correlation coefficient ( $R^2$ ) was found to range from 0.992 to 0.991, which is closer to unity. The computed values of  $q_e$  and the experimental  $q_e$  measurements are most well matched by the kinetic model. According to the findings, the copper adsorption mechanism. The results suggest that the copper adsorption mechanism on NZ followed the pseudo-second-order

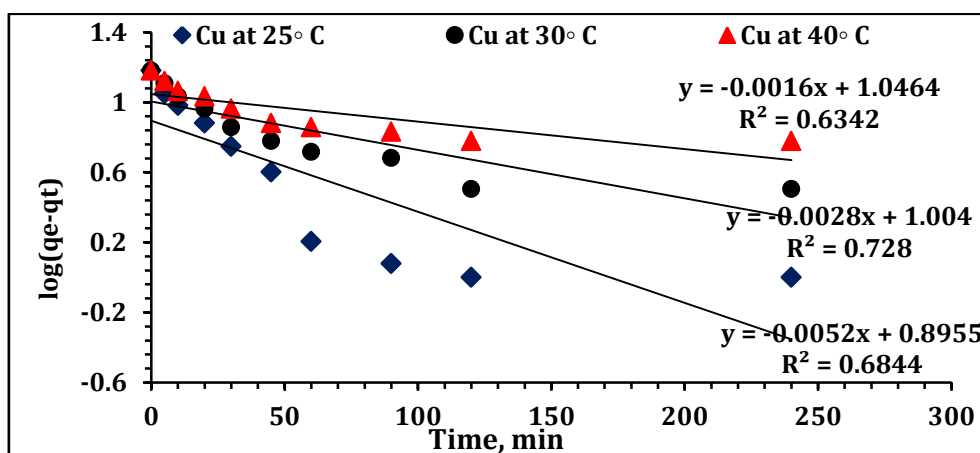


Fig. 12 A. Pseudo-first-order plot of copper adsorption on NZ

Table 2 Kinetic factors for copper adsorption onto NZ adsorbent

Temp, °C	Lagergren pseudo first-order				Pseudo second-order			
	$K_1(\text{min}^{-1})$	$q_{\text{ecal}}(\text{mg/g})$	$q_{\text{exp}}(\text{mg/g})$	$R^2$	$K_2(\text{min}^{-1})$	$q_{\text{ecal}}(\text{mg/g})$	$q_{\text{exp}}(\text{mg/g})$	$R^2$
25	0.033	14.4	21.34	0.962	0.0041	14.4	15.52	0.990
30	0.012	11.2	22.05	0.772	0.0043	11.2	12.00	0.990
40	0.007	7.6	22.89	0.588	0.0083	7.6	8.13	0.991

### Adsorption Isotherms

Adsorption isotherms play a significant role in determining NZ's maximum adsorption capacity. It was investigated how the relationship between the adsorption capacity of copper and its equilibrium concentration could be used to reconcile the experimental data of the adsorption isotherms generated from batch studies. The Langmuir and Freundlich isotherms are typically the most popular isotherm models for NZ applications in aqueous solutions. Langmuir and Freundlich's model (Saleem *et al.*, 2019; Espinoza-Sanches *et al.*, 2019; Haggag, 2021) measured the facts of equilibrium. The copper ion adsorption to ligand sites (NZ) in a single layer on the NZ surface is described by the Langmuir isotherm; the adsorption energy is constant and does not interact with the adsorbed species. Additionally, there is no copper migration in the surface plane. The Langmuir isotherm's linear form was represented by the following equation.

$$\frac{C_e}{q_e} = \frac{C_e}{q_{\text{max}}} + \frac{1}{K_L q_{\text{max}}}$$

$Q_{\text{max}}$  is the maximum saturation monolayer adsorption capacity (mg/g),  $K_L$  is the equilibrium adsorption constant (L/mg),  $C_e$  (mg/L) is the equilibrium copper concentration, and  $q_e$  (mg/g) is the equilibrium amount of copper adsorbed per unit mass of NZ. As shown in Fig. 13, the linear graph of  $C_e/q_e$  against  $C_e$  was used to determine  $q_{\text{max}}$  and  $K_L$ .

The Freundlich isotherm model, on the other hand, makes the assumption that as the active adsorption sites (NZ) become fully occupied, the energy of adsorption rapidly diminishes. The multilayer adsorption that takes place on the heterogeneous surface is controlled by the Freundlich isotherm, as is the interaction between the molecules that are adsorbed. The following is an expression for the Freundlich equation in linear form:

$$\text{Log} q_e = \text{Log} K_f + \frac{1}{n} \text{Log} C_e$$

Where  $q_e$  represents the equilibrium adsorption capacity (mg/g),  $C_e$  represents the equilibrium concentration of copper in solution (mg/L),  $K_f$

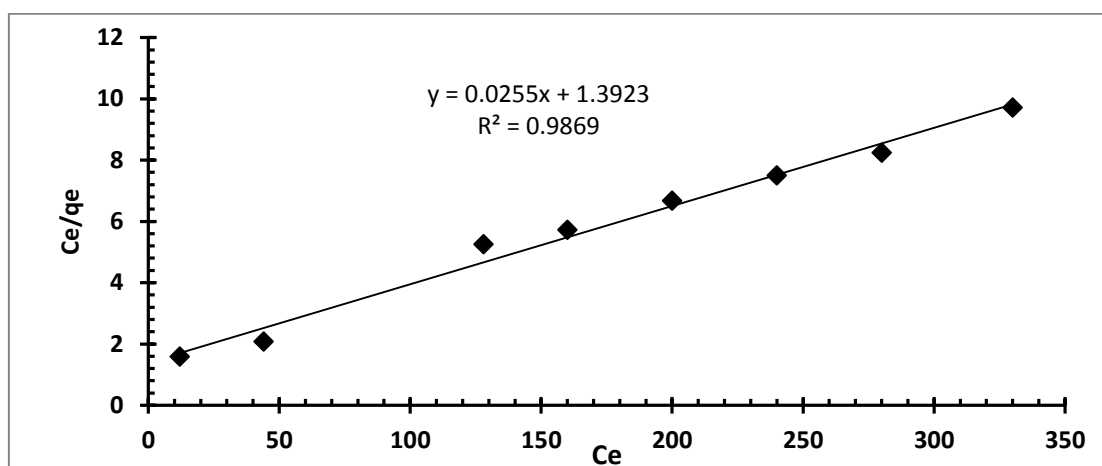


Fig. 13. Langmuir isotherm model of copper adsorption onto NZ

is Freundlich constant which represents the adsorption capacity, and  $n$  is Freundlich constant which represents adsorption intensity.  $K_F$  and  $n$  can be derived from the intercept and slope of the linear graph of  $\log q_e$  against  $\log C_e$  as illustrated in Fig. 14. The Langmuir and Freundlich constants are represented in Table 3.

According to the findings from the Langmuir and Freundlich isotherms equations, the copper adsorption on NZ correlates more strongly ( $R^2 > 0.9$ ) with the Langmuir equation than the Freundlich equation for the concentration range under consideration. The Freundlich isotherm model's  $K_f$  had a low value, and the  $n$  value indicated that the isotherm was insufficient to accurately depict copper's adsorption into NZ. The straight lines' maximum correlation coefficient  $R^2$  value was close to unity, which is an indication of a strong linear relationship according to the Langmuir isotherm model. Additionally, it was found that the intercept and slope of the Langmuir plot were 35.08 mg/g and 0.0124 L/mg, respectively. The NZ adsorbent's copper adsorption equilibrium must be determined. The Langmuir adsorption isotherm is followed by the utilized adsorption system, it has been found.

### Elution Experiments Studies

Using the following various eluents— $\text{CH}_3\text{COONa}$ ,  $\text{NaOH}$ ,  $\text{Na}_2\text{SO}_4$ ,  $\text{HNO}_3$ ,  $\text{H}_2\text{SO}_4$ ,  $\text{Na}_2\text{CO}_3$ , and  $\text{NaCl}$ —the regeneration and reuse from the loaded NZ have been studied. A batch procedure was used to carry out the copper elution at room temperature. For the elution

studies, 0.1 g of loaded NZ and 10 mL of 1 molar eluting fluid were shaken for an hour at 250 rpm. The results of copper desorption from the NZ using various solutions were thoroughly assessed and displayed in Table 4. From the results, it is clear that HCl, one of the eluents utilized in this investigation, had a favorable outcome. Washing metal-loaded NZ in ( $\text{HNO}_3$ ,  $\text{H}_2\text{SO}_4$ , and HCl) released 72.9%, 84.6%, and 93.8% of the metal, respectively, but the other eluents did not.

### Reusability Study Experiments

Utilizing NZ has the benefit of regeneration after reaching capacity. Reusability is the most important characteristic of an improved adsorbent for this use. NZ must be reusable for efficiency and originality, and because of the reversible adsorption process, it is possible to regenerate the adsorbent (Mahmoud *et al.*, 2015). Consequently, the cyclic adsorption-desorption investigation was conducted to determine the NZ adsorbent's reusability. The data in Table 5 revealed that the NZ's adsorption efficiency drastically declines with each cycle. The adsorbent still exhibits poor adsorption effectiveness even after 5 cycles. The outcomes demonstrated that it is feasible to remove copper from citrate solutions utilizing NZ adsorbents.

### Characterization of the Natural Zeolite

#### XRD analysis

The XRD patterns of the natural zeolite confirmed the mineralogy by using X ray Diffraction analysis which was applied to detect

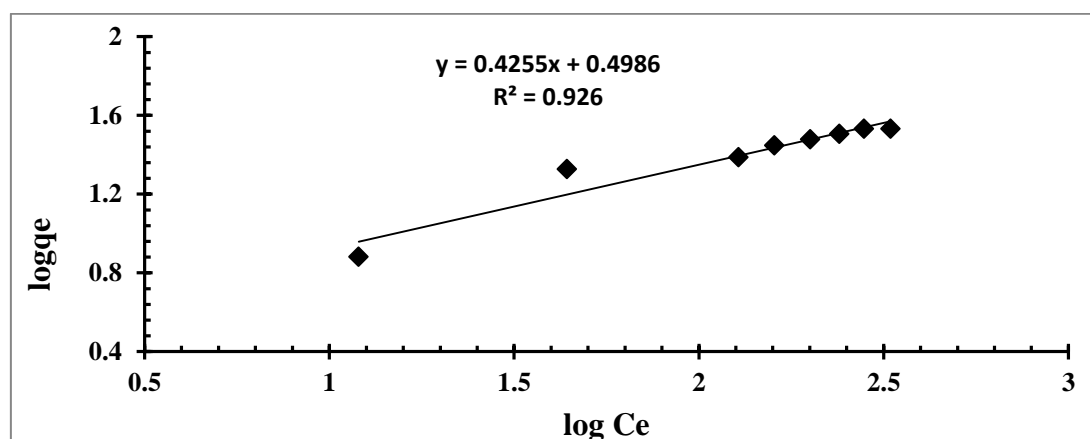


Fig. 14. Freundlich adsorption isotherm model of copper adsorption on NZ

Table 3. Langmuir and Freundlich constants for copper adsorption on NZ

Langmuir model parameters			Freundlich model parameters		
$q_{\max}$	$K_L$	$R^2$	$n$	$K_f$	$R^2$
35.08	0.0124	0.979	3.104	4.126	0.963

Table 4. Copper recovery from loaded NZ using different solutions

Eluent Type, 1.0 molar	Efficiency, %
H <sub>2</sub> SO <sub>4</sub>	84.6
HCl	93.8
HNO <sub>3</sub>	72.9
CH <sub>3</sub> COONa	28.5
Na <sub>2</sub> SO <sub>4</sub>	30.7
Na <sub>2</sub> CO <sub>3</sub>	42.8
NaOH	38.2

Table 5. Adsorption-desorption cycle for recovery of copper with NZ

No. of cycle	Sorption Efficiency, %	Desorption Efficiency, %
1	83.8	74.5
2	62.3	55.8
3	38.9	32.9
4	22.9	15.9
5	5.7	3.6

the crystallinity of the natural zeolite. The NZ powder showed sharp feature peaks around  $2\theta = 7.1^\circ, 20.3^\circ, 38.5^\circ, 58.4^\circ$  and  $65.9^\circ$  were attributed to the crystalline structure of the NZ powder as shown in Fig. 15

#### Energy dispersive X-ray (EDX) spectroscopy and Surface Morphology Studies of NZ

To evaluate the chemical composition (elemental analysis) before and after loading the copper ion, EDX and analysis of NZ were performed. Prior to loading, the natural zeolites were examined by EDX and were found to mostly include Si, Na, and Al, as shown in Fig. (16A). EDX analysis of NZ following copper ion adsorption revealed the presence of Na, Si, Fe, K, and Cu. The outcomes supported NZ's adsorption of copper as shown in Fig. 16B.

#### Characterization of the Soil

##### XRD analysis

The soil's XRD diffraction patterns, which were used to determine the soil's crystallinity, confirmed the mineralogy. The soil powder displayed prominent feature peaks at  $28.1^\circ, 32.3^\circ, 40.5^\circ,$  and  $55.4^\circ$ , which were attributed to the soil powder's crystalline structure as depicted in Fig. 17.

##### Energy dispersive X-ray (EDX) spectroscopy and Surface Morphology Studies of soil

analyzing the elements to establish the chemical makeup both before and after the copper ion is loaded, EDX and soil analysis were completed. According to Fig. 18A, the natural zeolites were tested by EDX prior to loading and are mostly composed of Mg, Si, K,

Fe, and Al. By using EDX to evaluate the soil after copper ion adsorption, it was discovered that Mg, Si, Fe, K, Al, and Cu were present. The outcomes validated the copper absorption by soil shown in Fig. 18B.

Fig. 18A, B's SEM images Showcase the copper adsorption arrangement before and after. Because of the soil's porous surface morphology, the copper molecules can penetrate into the soil and cause swelling. This often means that the porous nature of the structured soil favors the adsorption of copper from aqueous solutions. The copper solution was then thoroughly applied to the soil's surface and dispersed throughout the ground.

#### Conclusions

This study has looked into the use of citric acid solution to leach copper from polluted soil. The findings demonstrated that the reaction rate rises with time, hydrogen ion  $[H^+]$  concentration, liquid/solid mass ratio, and leaching temperature whereas the leaching rate is very marginally influenced by stirring speed. Scanner electron microscopy (SEM) and X-ray diffraction (XRD) were used to characterize natural zeolite. Copper adsorption from citrate solution has been investigated in NZ. The Langmuir isotherm model was successfully used to fit the maximal monolayer adsorption capacity,  $q_{max} = 34.0$  mg Cu/g NZ at pH 3.0 for 90 minutes of contact time at room temperature. A pseudo-second-order rate equation is obeyed by the adsorption kinetics process. Using 1 M HCl, 93.8% of the copper from the NZ was successfully desorption.

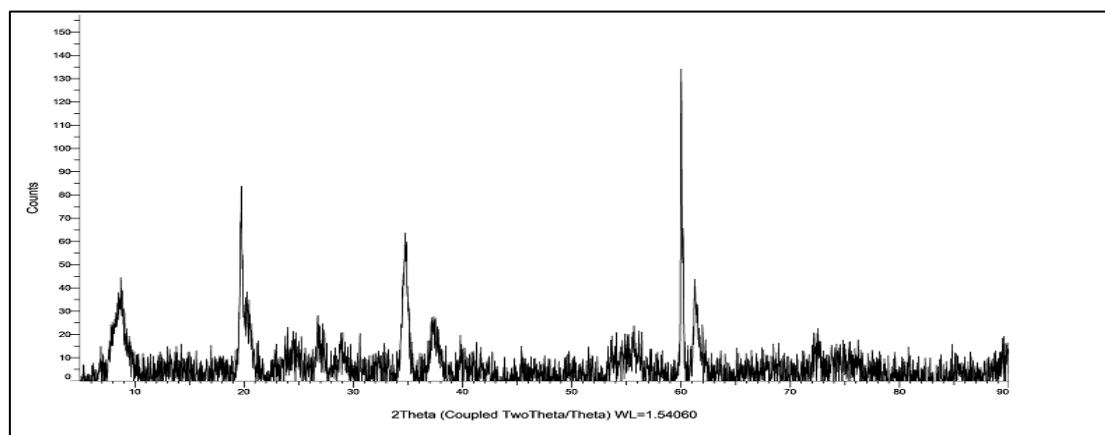


Fig. 15. XRD patterns of NZ before copper adsorption

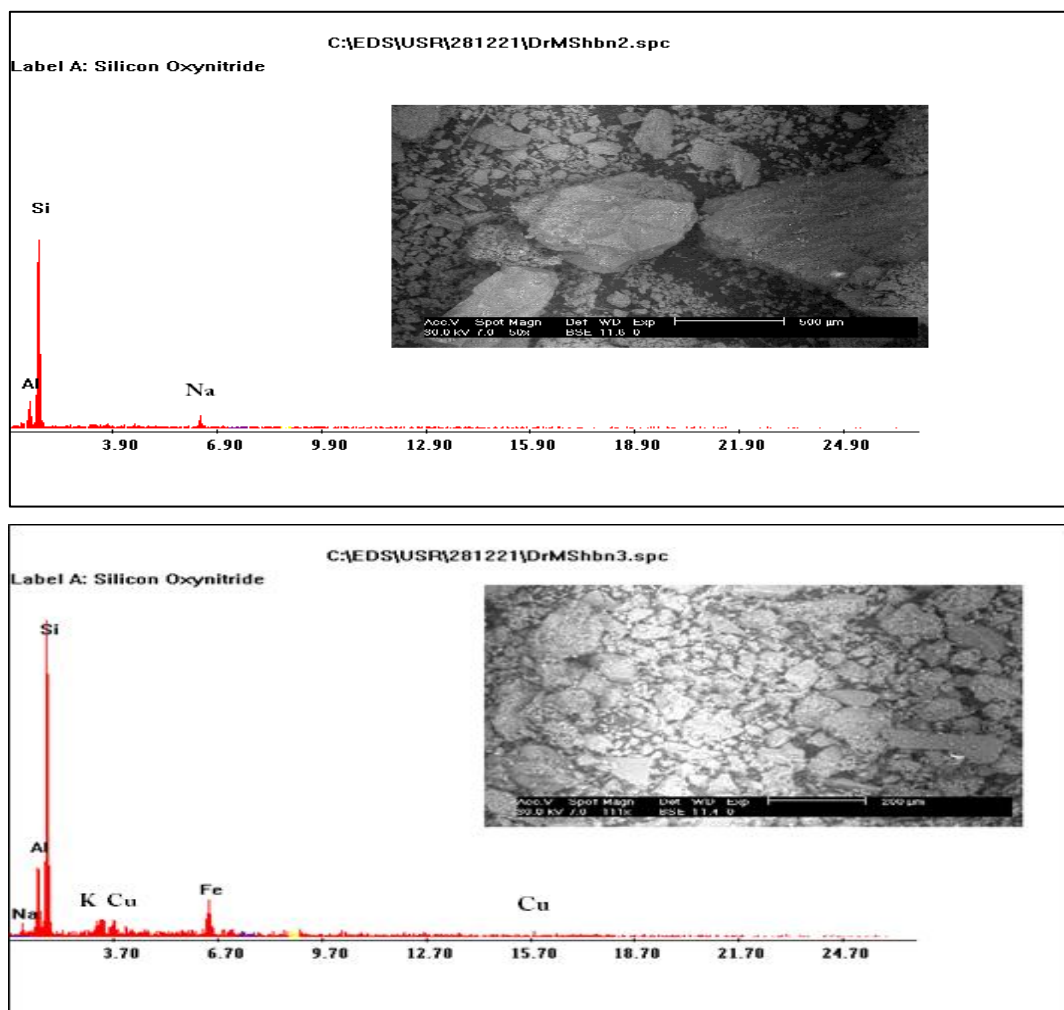


Fig. 16. EDX spectrum and SEM images of NZ (A) before copper adsorption and (B) after adsorption of copper

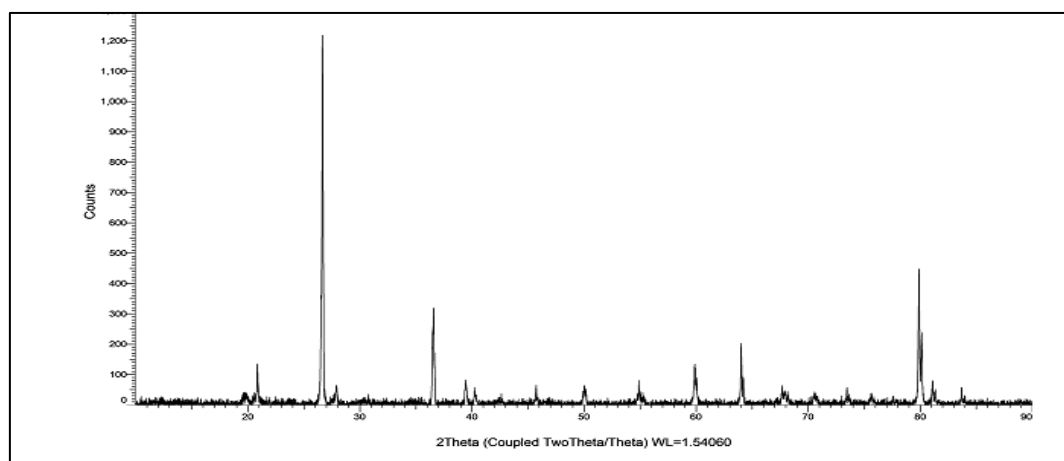


Fig. 17. XRD patterns of soil before copper adsorption

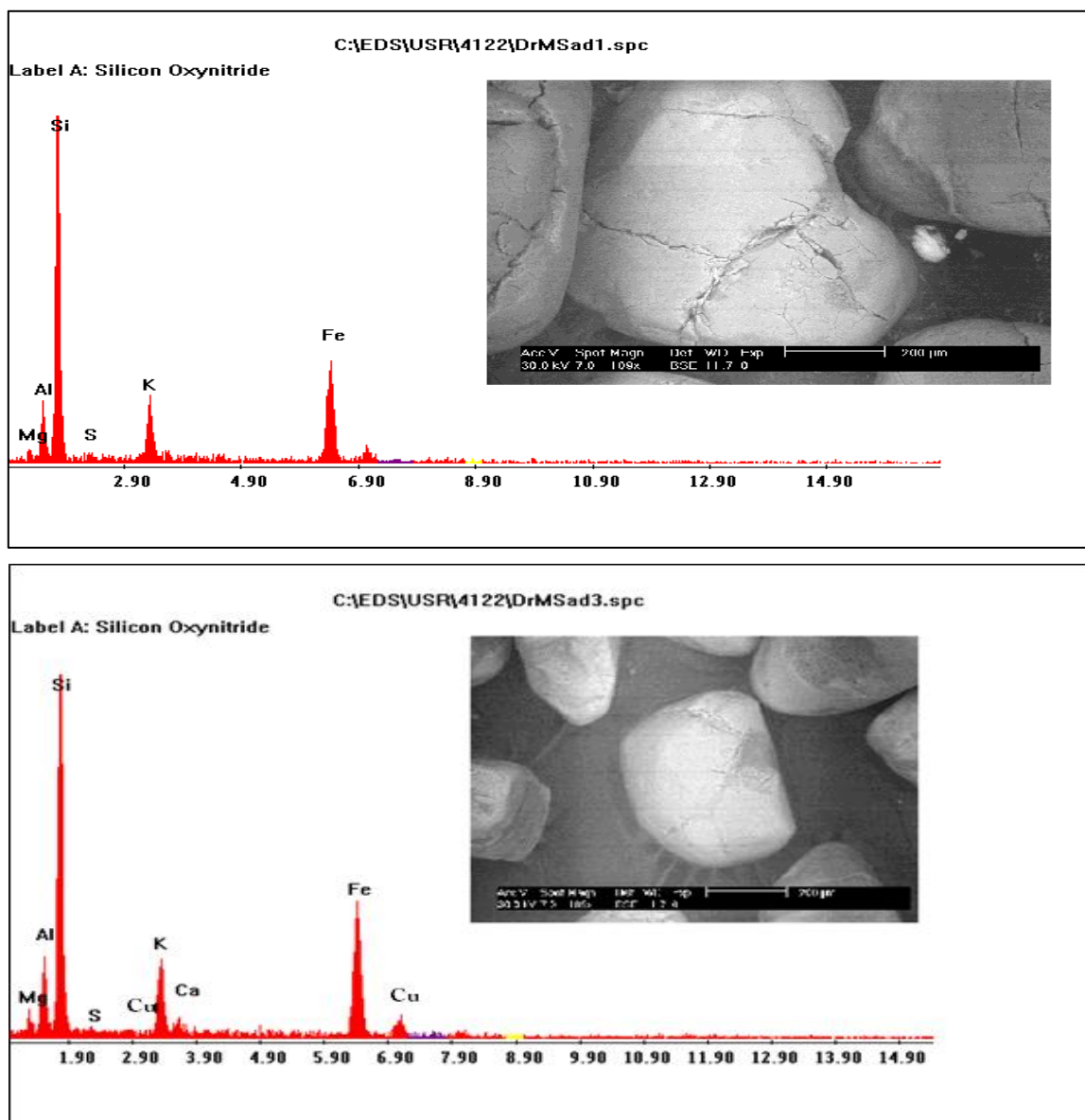


Fig. 18. EDX spectrum and SEM images of soil (A) before copper adsorption and (B) after adsorption of copper

## REFERENCES

- Abdel-Samad, A.A., M.M. Abdel Aal, E.A. Haggag and W.M. Yosef (2020). Synthesis and characterization of functionalized activated carbon for removal of uranium and iron from phosphoric acid. *J. Basic and Environ. Sci.*, 7: 140-153.
- Akyıl, S., M.A. Aslani and Ş.Ö. Aytaş (1998). Distribution of uranium on zeolite X and investigation of thermodynamic parameters for this system. *J. Alloys and Comp.*, 271: 769-773.
- Ames, L.L., J.E. McGarrah and B.A. Walker (1983). Sorption of trace constituents from aqueous solutions onto secondary minerals. I. Uranium. *Clays and Clay Minerals*, 31(5): 321 - 334.
- Babel, S. and T.A. Kurniawan (2003). Low-cost adsorbents for heavy metals uptake from contaminated water: a review. *J. Hazardous Materials*, 97 (1-3): 219-243.

- Chauhan, G.S., S. Mahajan and L.K. Guleria (2000). Polymers from renewable resources: sorption of Cu<sup>2+</sup> ions by cellulose graft copolymers. *Desalination*, 130(1): 85-88.
- Dacrory, S., E.S. Haggag, A.M. Masoud, S.M. Abdo, A.A. Eliwa and S. Kamel (2020). Innovative synthesis of modified cellulose derivative as a uranium adsorbent from carbonate solutions of radioactive deposits. *Cellulose*, 1-16.
- Donia, A.M., A.A. Atia, E.M. Moussa, A.M. El-Sherif and M.O. Abd El-Magied (2009). Removal of uranium (VI) from aqueous solutions using glycidyl methacrylate chelating resins. *Hydrometallurgy*, 95 (3-4): 183-189.
- El-Sheikh, A.S., E.A. Haggag and N.R. Abd El-Rahman (2020). Adsorption of Copper from Sulfate Medium Using a Synthetic Polymer; Kinetic Characteristics, *Radiochem.*, doi.org 10.1134/S1066362220040074, 62 (4):499-510.
- Espinoza-Sanchez, M.A., K. Arevalo-Nino, I. Quintero-Zapata, I. Castro-Gonzalez and V. Almaguer-Cantu (2019). Cr (VI) adsorption from aqueous solution by fungal bioremediation based using *Rhizopus* sp. *J. Environ. Manag.*, 251: 109595.
- Ganesh, R., K.G. Robinson, L. Chu, D. Kucsmas and G.D. Reed (1999). Reductive precipitation of uranium by *Desulfovibrio desulfuricans*: evaluation of cocontaminant effects and selective removal. *Water Res.*, 33 (16): 3447-3458.
- Gharabaghi, M., M. Noaparast and M. Irannajad (2009). Selective leaching kinetics of low-grade calcareous phosphate ore in acetic acid. *Hydrometallurgy*, 95(3-4): 341-345.
- Gupta, V.K. and A. Rastogi (2008). Biosorption of lead (II) from aqueous solutions by non-living algal biomass *Oedogonium* sp. and *Nostoc* sp.-a comparative study. *Colloids and Surfaces B: Biointerfaces*, 64 (2): 170-178.
- Haggag, E.A. (2021). Cellulose hydrogel for enhanced copper (VI) capture from nitrate medium: preparation, characterisation and adsorption optimization. *Int. J. Environ. Anal. Chem.*, DOI: 10.1080/03067319.2021.2005791
- Haggag, E.S.A., M.S. Khalafalla and A.M. Masoud (2021a). Leaching kinetics of uranium, rare earth elements and copper using tartaric acid from El Allouga ore material, Southwestern Sinai, Egypt. *Int. J. Environ. Anal. Chem.*, 1-16.
- Haggag, E.A., A.A. Abdelsamad, M.B. Masod, M.M.E. Mohamed and A. Mohamed (2021b). Kinetic studies on the adsorption of copper on a mesoporous impregnated activated carbon, *Egypt. J. Chem.*, 64 (3): 1371-1385. DOI:10.2608/EJCHEM.2020.50611.3039
- Haggag, E.A., A.A. Abdelsamad and A.M. Masoud (2019). Potentiality of copper extraction from acidic leach liquor by polyacrylamide-acrylic acid titanium silicate composite adsorbent. *Int. J. Environ. Anal. Chem.*, July,doi.org/10.1080/03067319.2019.1636037
- Higgins, J.B., R.B. LaPierre, J.L. Schlenker, A.C. Rohrman, J.D. Wood, G.T. Kerr and W.J. Rohrbaugh (1988). The framework topology of zeolite beta. *Ame. Chem. Soci., Division of Petroleum Chem., Preprints (USA)*, 33(CONF-880939-).
- Kadous, A., M. Didi and D. Villemin (2009). Extraction of Uranium (VI) using D2EHPA/TOPO based supported liquid membrane. *J. Radioanalytical and Nuclear Chem.*, 280(1), 157-165.
- Khawassek, Y.M., E.A. Gawad, E.A. Haggag and A.A. Eliwa (2015). Kinetics of Leaching Process of REE from El-Missikat Shear Zone Eastern Desert, Egypt. *J. Chem. Technol.*, 10 (6): 295-306.
- Khawassek, Y.M., A.A. Eliwa, E.A. Haggag, S.A. Mohamed and S.A. Omar (2017). Equilibrium, Kinetic and Thermodynamics of Copper Adsorption by Ambersep 400 SO<sub>4</sub> Resin, *Arab J. Nuclear Sci. and Applic.*, 50 (4): 100-112, Web site: esnsa-eg.com.
- Khawassek, Y.M., A. Haggag, S.A. Mohamed and S.A. Omar (2016). Kinetics leaching process of uranium ions from El-Erediya rock by sulfuric acid solution. *Int. J. Nuclear Energy Sci. and Eng.*, 6: 35-48.
- Kilincarslan, A. and S. Akyil (2005). Uranium adsorption characteristic and thermodynamic



- behavior of clinoptilolite zeolite. *J. Radioanal. and Nuclear Chem.*, 264 (3): 541-548.
- Kim, M.S., K.M. Hong and J.G. Chung (2003). Removal of Cu (II) from aqueous solutions by adsorption process with anatase-type titanium dioxide. *Water Res.*, 37 (14): 3524-3529.
- Kocaoba, S., Y. Orhan and T. Akyüz (2007). Kinetics and equilibrium studies of heavy metal ions removal by use of natural zeolite. *Desalination*, 214 (1-3): 1-10.
- Krestou, A., A. Xenidis and D. Papias (2003). Mechanism of aqueous uranium (VI) uptake by natural zeolitic tuff. *Minerals Eng.*, 16 (12): 1363-1370.
- Kryvoruchko, A.P., L.Y. Yurlova, I.D. Atamanenko and B.Y. Kornilovich (2004). Ultrafiltration removal of U (VI) from contaminated water. *Desalination*, 162: 229-236.
- Kundu, S. and A.K. Gupta (2005). Analysis and modeling of fixed bed column operations on As (V) removal by adsorption onto iron oxide-coated cement (IOCC). *J. Colloid and Interface Sci.*, 290 (1): 52-60.
- Lagergren, S. (1898). Zur theorie der sogenannten adsorption gelöster stoffe. *Kungliga svenska vetenskapsakademiens. Handlingar*, 24, 1-39.
- Liu, Y., M. Chen and H. Yongmei (2013). Study on the adsorption of Cu (II) by EDTA functionalized Fe<sub>3</sub>O<sub>4</sub> magnetic nano-particles. *Chem. Eng. J.*, 218: 46-54.
- Loizidou, M. and R.P. Townsend (1987). Ion-exchange properties of natural clinoptilolite, ferrierite and mordenite: Part 2. Lead-sodium and lead-ammonium equilibria. *Zeolites*, 7 (2): 153-159.
- Mahmoud, M.A., E.A. Gawad, E.A. Hamoda and E.A. Haggag (2015). Kinetics and thermodynamic of Fe (III) adsorption type onto activated carbon from biomass: kinetics and thermodynamics studies, 22: 23.
- Marczenko, Z. and M. Balcerzak (2000). Separation, preconcentration and spectrophotometry in inorganic analysis. Elsevier.
- Mellah, A., S. Chegrouche and M. Barkat (2006). The removal of uranium (VI) from aqueous solutions onto activated carbon: kinetic and thermodynamic investigations. *J. Colloid and Interface Sci.*, 296 (2): 434-441.
- Moussa, M.A., A.M. Daher, S.A. Omar, Y.M. Khawassek, E.A. Haggag and E.A. Gawad (2014). Kinetics of leaching process of Uranium from EL-Missikat shear zone Eastern Desert, Egypt. *J. Basic and Environ. Sci.*, 1 : 65-75.
- Panuccio, M.R., F. Crea, A. Sorgonà and G. Cacco (2008). Adsorption of nutrients and cadmium by different minerals: Experimental studies and modelling. *J. Environ. Manag.*, 88 (4): 890-898.
- Perić, J., M. Trgo and N.V. Medvidović (2004). Removal of zinc, copper and lead by natural zeolite-a comparison of adsorption isotherms. *Water Res.*, 38(7): 1893-1899.
- Puigdomenech, I. (2006). HYDRA (hydrochemical equilibrium-constant database) and MEDUSA (make equilibrium diagrams using sophisticated algorithms) programs. Royal Inst. Technol., Sweden. <http://www.kemi.kth.se/medusa>
- Ren, Y., N. Li, J. Feng, T. Luan, Q. Wen, Z. Li, and M. Zhang (2012). Adsorption of Pb (II) and Cu (II) from aqueous solution on magnetic porous ferrosin MnFe<sub>2</sub>O<sub>4</sub>. *J. Colloid and Interface Sci.*, 367 (1): 415-421.
- Saleem, J., U.B. Shahid, M. Hijab, H. Mackey and G. McKay (2019). Production and applications of activated carbons as adsorbents from olive stones. *Biomass Conversion and Biorefinery*, 9(4): 775-802.
- Shadbad, M.J., A. Mohebbi and A. Soltani (2011). Mercury (II) removal from aqueous solutions by adsorption on multi-walled carbon nanotubes. *Korean J. Chem. Eng.*, 28 (4): 1029-1034.
- Sharma, P. and R. Tomar (2008). Synthesis and application of an analogue of mesolite for the removal of uranium (VI), thorium (IV), and europium (III) from aqueous waste. *Microporous and Mesoporous Materials*, 116 (1-3): 641-652.

- Sprynskyy, M., B. Buszewski, A.P. Terzyk and J. Namieśnik (2006). Study of the selection mechanism of heavy metal (Pb<sup>2+</sup>, Cu<sup>2+</sup>, Ni<sup>2+</sup>, and Cd<sup>2+</sup>) adsorption on clinoptilolite. *J. Colloid and Interface Sci.*, 304(1): 21-28.
- Thanavel, M., S.K. Kadam, S.P. Biradar, S.P. Govindwar, B.H. Jeon and S.K. Sadasivam (2019). Combined biological and advanced oxidation process for decolorization of textile dyes. *SN Appl. Sci.*, 1(1): 1-16.
- Wu, X.L., D. Zhao and S.T. Yang (2011). Impact of solution chemistry conditions on the sorption behavior of Cu (II) on Lin'an montmorillonite. *Desalination*, 269 (1-3): 84-91.
- Zafar, Z.I. and M. Ashraf (2007). Selective leaching kinetics of calcareous phosphate rock in lactic acid. *Chem. Eng. J.*, 131 (1-3): 41-48.
- Zhao, G., H. Zhang, Q. Fan, X. Ren, J. Li, Y. Chen and X. Wang (2010). Sorption of copper (II) onto super-adsorbent of bentonite-polyacrylamide composites. *J. Hazardous Materials*, 173 (1-3): 661-668.
- Zhu, C., F. Liu, C. Xu, J. Gao, D. Chen and A. Li (2015). Enhanced removal of Cu (II) and Ni (II) from saline solution by novel dual-primary-amine chelating resin based on anion-synergism. *J. Hazardous Materials*, 287: 234-242.
- Zhu, J., V. Cozzolino, M. Fernandez, R.M.T. Sánchez, M. Pigna, Q. Huang and A. Violante (2011). Sorption of Cu on a Fe-deformed montmorillonite complex: Effect of pH, ionic strength, competitor heavy metal, and inorganic and organic ligands. *Appl. Clay Sci.*, 52 (4): 339-344.
- Zou, W., H. Bai, L. Zhao, K. Li and R. Han (2011). Characterization and properties of zeolite as adsorbent for removal of uranium (VI) from solution in fixed bed column. *J. Radioanal. and Nuclear Chem.*, 288 (3): 779-788.

## إزالة النحاس من المحلول المائي للتربة الملوثة باستخدام الزيوليت الطبيعي

أحمد سعد عبدالعزيز<sup>1</sup> – خالد جودة سليمان<sup>2</sup> – محمد شعبان عتريس<sup>1</sup>

1- هيئة المواد النووية – مصر

2- قسم الأراضي – كلية الزراعة – جامعة الزقازيق - مصر

الزيوليت كمادة ماصة منخفضة التكلفة لإزالة النحاس من المحلول المائي تحت تأثير معاملات العملية المختلفة مثل الرقم الهيدروجيني للوسيط، ووقت التلامس، ودرجة حرارة الامتزاز، وتركيز النحاس الأولي ونسبة S/L. تم تحديد التوازن والخصائص الحركية للزيوليت من الوسط الحمضي. كان الغرض من هذا التحقيق هو تقييم امتزاز النحاس من التربة الملوثة بها مسبقاً وكذلك إزالتها باستخدام محاليل مختلفة. تم استخدام الأحماض العضوية الضعيفة الستريك، المالك، السكسينيك، الطرطريك، اللاكتيك والأكساليك لإزالة المعادن من التربة عن طريق الغسيل. جمعت عينات التربة من الطبقة السطحية (0 - 30 سم) في حقل إنشاص بمحافظة الشرقية، مصر. كانت التربة ملوثة مسبقاً بـ 100 جزء في المليون من سترات النحاس. تضمنت التجربة استخدام الأحماض العضوية الضعيفة بكميات تتراوح من 0.5 إلى 3.0% لتقييم كفاءة الترشيح للنحاس. تم العثور على قدرة الامتزاز العملية للنحاس على الزيوليت في ظل الظروف المثلى لتصل إلى 32 مجم/جم والتي تتطابق مع 32 mg / g Langmuir isotherm. تم أيضاً تحديد المعلمات الفيزيائية بما في ذلك حركية الامتزاز ونماذج متساوي الحرارة والبيانات الديناميكية الحرارية لوصف طبيعة امتزاز النحاس بواسطة الزيوليت الطبيعي. وجد أن الزيوليت الطبيعي العامل يتفق مع كل من تفاعل الدرجة الثانية الزائف ونموذج لانجموير.

المحكمون:

1- أ.د. ياسر خواسك

2- أ.د. أيمن محمود حلمي

رئيس بحوث هيئة المواد النووية

أستاذ ورئيس قسم الأراضي – كلية الزراعة – جامعة الزقازيق.